HHS Public Access

Author manuscript

Clin Cancer Res. Author manuscript; available in PMC 2017 December 15.

Published in final edited form as:

Clin Cancer Res. 2016 December 15; 22(24): 6176–6191. doi:10.1158/1078-0432.CCR-15-3107.

BMI-1 targeting interferes with patient-derived tumor-initiating cell survival and tumor growth in prostate cancer

Nitu Bansal[#1], **Monica Bartucci**[#1], **Shamila Yusuff**[1], **Stephani Davis**[2], **Kathleen Flaherty**[1], **Eric Huselid**[2], **Michele Patrizii**[2], **Daniel Jones**[3], **Liangxian Cao**[4], **Nadiya Sydorenko**[4], **Young-Choon Moon**[4], **Hua Zhong**[5], **Daniel J. Medina**[1,6], **John Kerrigan**[1], **Mark N. Stein**[1,6], **Isaac Y. Kim**[1,7], **Thomas W. Davis**[4], **Robert S. DiPaola**[1,6], **Joseph R. Bertino**[1,2,6,*], and **Hatem E. Sabaawy**[1,2,3,6,*]

[1]Rutgers Cancer Institute of New Jersey, Rutgers University, New Brunswick, NJ 08901.

[2]Graduate Program in Cellular and Molecular Pharmacology, Rutgers University, New Brunswick, NJ 08901.

[3]Graduate Program in Cell and Developmental Biology, RBHS-Robert Wood Johnson Medical School, Graduate School of Biomedical Sciences, Rutgers University, New Brunswick, NJ 08901.

[4]PTC Therapeutics, Inc., 100 Corporate CT, South Plainfield, NJ 07080.

[5]Department of Pathology and Laboratory Medicine, Rutgers University, New Brunswick, NJ 08901.

[6]Department of Medicine, Rutgers University, New Brunswick, NJ 08901.

[7]Department of Surgery, RBHS-Robert Wood Johnson Medical School, Rutgers University, New Brunswick, NJ 08901.

[#] These authors contributed equally to this work.

Abstract

Purpose—Current prostate cancer (PCa) management calls for identifying novel and more effective therapies. Self-renewing tumor-initiating cells (TICs) hold intrinsic therapy-resistance and account for tumor relapse and progression. As BMI-1 regulates stem cell self-renewal, impairing BMI-1 function for TICs-tailored therapies appears to be a promising approach.

Experimental design—We have previously developed a combined immunophenotypic and time-of-adherence assay to identify CD49b^{hi}CD29^{hi}CD44^{hi} cells as human prostate TICs. We utilized this assay with patient derived prostate cancer cells and xenograft models to characterize the effects of pharmacological inhibitors of BMI-1.

Results—We demonstrate that in cell lines and patient-derived TICs, BMI-1 expression is upregulated and associated with stem cell-like traits. From a screened library, we identified a number of post-transcriptional small molecules that target BMI-1 in prostate TICs.

[*]Corresponding authors: J R Bertino, M.D., Cancer Institute of New Jersey, 195 Little Albany Street, Room 3033, New Brunswick, NJ 08901, USA. Telephone: 732-235-8510, bertinoj@cinj.rutgers.edu; H E Sabaawy, M.D., Ph.D., Cancer Institute of New Jersey, 195 Little Albany Street, Room 4557, New Brunswick, NJ 08901, USA. Telephone: 732-235-8081, sabaawhe@cinj.rutgers.edu.

COI statement: “The authors disclose no potential conflicts of interest.”

Pharmacological inhibition of BMI-1 in patient-derived cells significantly decreased colony formation *in vitro* and attenuated tumor initiation *in vivo*, thereby functionally diminishing the frequency of TICs, particularly in cells resistant to proliferation- and androgen receptor (AR)-directed therapies, without toxic effects on normal tissues.

Conclusions—Our data offer a paradigm for targeting TICs and support the development of BMI-1-targeting therapy for a more effective PCa treatment.

Keywords

Prostate cancer stem cells; tumor-initiating cells; BMI-1; zebrafish

Introduction

Prostate cancer (PCa) is the most common cancer affecting men in the developed world (1). Current therapies including androgen deprivation (ADT) and androgen receptor (AR) directed therapies are only temporarily effective, and therapy resistance and relapse are commonly inevitable (2). We and others have shown that primary PCa contain cells endowed with self-renewal and tumorigenic potential (3-8), known as tumor-initiating cells (TICs) (9). By virtue of their resistance to therapy, TICs could be the prime cause of tumor relapse. Thus, in order to accomplish tumor eradication, efforts are made to design TIC-tailored therapy that would selectively target these highly aggressive tumorigenic cells.

An attractive treatment strategy is to use agents capable of impeding the self-renewal abilities of TICs, therefore targeting heterogeneous cells in all tumor clone(s) within a given patient. BMI-1 (B-cell specific MMLV insertion site-1), a member of the polycomb family of the chromatin remodeling complex, was shown to regulate stem cell self-renewal (10) and play a key role in PCa initiation and progression (11). In clinical specimens, BMI-1 expression correlates with high rates of PCa recurrence (12), and downstream targets of the BMI-1 are associated with therapy-resistant PCa (13). These data closely associate BMI-1 with the presence of tumor-initiating stem-like cells in clinical PCa samples, making it reasonable to assume that small-molecule inhibitors targeting BMI-1 could be the first in a new class of antitumor therapy directed against self-renewing and chemo-resistant TICs.

Previously, we developed a surrogate self-renewal assay that allowed us to isolate TICs from PCa tissue based on α2β1-integrin (also called CD49b/CD29) and CD44 protein expression (6). Herein, we demonstrate that in prostate TICs, BMI-1 is overexpressed and functionally regulates their survival and maintenance. Targeting of BMI-1 with a novel inhibitor impaired self-renewal and migratory potential *in vitro.* Consistently, BMI-1 inhibition *in vivo* decreased tumor growth and significantly reduced TICs in patient-derived samples and tumor xenografts, as evaluated by CD49b/CD29/CD44 staining, serial transplantation *in vivo* and clonogenic prostasphere assays *ex-vivo.* Remarkably, these outcomes were not observed following conventional chemotherapy treatments while targeting BMI-1 also inhibited PCa cells resistant to AR directed therapies. Given the role of TICs in therapy resistance, these observations support the evaluation of BMI-1 inhibitors for a more effective PCa management.

Materials and Methods

Materials

Initial small molecule inhibitors were from PTC therapeutics, South Plainfield, NJ. C-209 was latter synthetized and purified by the Chemistry Department at Rutgers University. Docetaxel (also called taxotere), doxorubicin, and methotrexate were from Rutgers Cancer Institute of New Jersey (CINJ) pharmacy. Cycloheximide was purchased from Cell Signaling. Collagen-I was bought from BD Biosciences, and NOD/SCID/IlRγ mice were from the Jackson laboratory.

Collagen adherence assay

Putative cancer stem-like cells, or TICs, were isolated by combining phenotypic analyses (3) with collagen adherence as described (6). Briefly, tissue culture dishes were coated with 70 μg/ml of collagen-I for 1 hr at room temperature or overnight at 4°C. Subsequently, plates were washed with PBS and blocked in 0.3% BSA for 30 minutes. Cells were plated on collagen plates for 5 or 20 minutes. Next, cells adhering in 5 minutes and not adhering after 20 minutes were collected and used for further experiments.

Identification of BMI-1 post-transcriptional inhibitors

We have previously examined a small molecule library (PTC therapeutics) for post-transcriptional inhibitors of BMI-1 utilizing luciferase reporters encompassing the 5‘UTR and 3‘UTR of human BMI-1 (14). Anti-BMI-1 antibody (Millipore, clone F6) was used for ELISA assays and western blotting (WB). The principal BMI-1's downstream target, mono-ubiquitinated (γ) histone H2A, was examined using a mouse monoclonal anti-ubiquityl-histone H2A antibody (clone E6C5) (Millipore). The selectivity of C-209 was further investigated by profiling it against both a library of purified protein kinase targets using the Z’-LYTE SelectScreen profiling activity assay (Invitrogen) against 245 kinases at [ATP] Km and C-209 (3μM), and a phosphatase profiler assay with an IC_{50} profiler (Millipore). Both assays yielded <10% activity for C-209.

Electrostatic potential and docking of C-209 to the human BMI-1 RNA

All quantum mechanics calculations were performed using Gaussian 09. C-209 was geometry optimized at the PM6 level using tight convergence. A single- point energy calculation at the B3LYP/6- 31G(d) level was performed and Merz-Kollman partial atomic charges were estimated from the electrostatic potential. The reported energy is gas phase. The surface and contour plot was prepared using the GaussView program. The electrostatic potential allowed us to build a model for docking (15) of C-209 to the human BMI RNA. We used the UCSF DOCK program (v6.7). The small molecule C-209 was built using the Spartan (Wavefunction, Inc) quantum mechanics package and geometry optimized at the PM6 semi-empirical level. The Amber99SB partial atomic charges were used on the RNA and AM1-BCC partial atomic charges were calculated for C-209 within the UCSF Chimera molecular graphics package (15). The interaction energy scores (E_{int}) estimate the binding energy in the DOCK scoring of C-209 with BMI-1 RNA, using guanine as a reference. DOCK scores, E_{vdw} (kcal/mol), E_{elec} (kcal/mol), and E_{int} (kcal/mol), were generated using

the following equation: $E_{int} = E_{vdw} + E_{elec}$. C-209 DOCK scores were E_{vdw} (kcal/mol) −60.6, E_{elec} (kcal/mol) −5.2, and E_{int} (kcal/mol) −65.8, as compared to guanine scores of E_{vdw} (kcal/mol) −36.4, E_{elec} (kcal/mol) −4.1, and E_{int} (kcal/mol) −40.5. The lower the energy score; the more stable the complex contacts with the RNA due to complete fitting into the binding pocket.

Patient-derived cell culture

Primary normal and PCa cells were isolated from specimens obtained at Rutgers CINJ in accordance with an Institutional Review Board (IRB)-approved protocol and upon informed consent from patients undergoing surgical resection. Normal and tumor samples were each extracted from the same patient as adjacent tissues examined and verified following pathological examination. For cell isolation from surgical specimen, tissue was minced into small pieces and incubated with 1× collagenase (Sigma Aldrich) for 2 to 4 hours depending on the size of the tissue. After incubation, the dissociated pieces were strained with a 70μm filter to remove debris and the dissociated cells were washed with PBS at 250g for 2 minutes in order to eliminate fibroblasts. The recovered cells were cultured in prostate epithelial basal media (PrEBM, Lonza) for at least 14 days before being used for experiments at low passage numbers. Cells from immortalized PCa lines were maintained at low passage numbers in RPMI media (GIBCO), 10% fetal bovine serum, and 1% penicillin-streptomycin. TICs, obtained from DU145 cells after selection (6), were maintained in keratinocyte serum free medium (KSFM) supplemented with epidermal growth factor (EGF) and bovine pituitary extract (KSFM media) (All from Invitrogen). Protein analyses, flow cytometry, cell sorting, cell viability and survival assays, and cell migration assays are described in further detail in the Supplementary Methods.

Spheroid forming assay

We have previously characterized spheroid forming (prostasphere) abilities from multiple PCa cell lines and primary cells (6). To measure prostasphere forming abilities, 2×10^3 cells/well were suspended in KSFM media and plated on 1% agarose coated plates. Every 3 days, half of the media was replaced and prostaspheres of >50 μm in diameter and consisting of >50 cells were counted on day14. Single cells from day-7 spheroids were used in secondary and tertiary spheroid assays. Colony forming abilities of PCa cells plated at 1×10^3 cells/well in six-well dishes coated with 1% agar were performed as described (16). Methotrexate (10nM), Doxorubicine (50nM) and Cyclohexamide (10μg/ml) were employed. The prostasphere and colony forming assays are described in further details in the Supplementary Methods.

Luciferase target assay

Cells were transfected with Lipofectamine 2000 (Invitrogen) using the following plasmids: pCDNA3.1+Luc Vector UTR, pCDNA3.1+Luc BMI-1 3'UTR, pCDNA3.1+ Luc BMI-1 5'UTR, and pCDNA3.1+Luc BMI-1 5'&3'UTR as previously described (14). To normalize the transfection efficiency, cells were transfected with pCMV-AcGFP1 at a ratio of 1/3 along with the UTR plasmids. Cells were then visually counted for GFP^+ cells. After 19 hours, 5,000 cells/well were seeded in a 96 well plate and 6 hrs later, C-209 was added. At 24 hours post-treatment, cells were assayed for luciferase activity using Steady-Glo system

(Promega). For QPCR, total RNA was extracted using TRIzol Reagent (Life Technologies) and purification was assessed with RNeasy plus Mini kit (Qiagen). cDNA was synthesized from 100 ng of total RNA using SuperScript® VILO™ cDNA Synthesis Kit (Life Technologies) according to the manufacturer's instruction. Synthesized cDNAs (10ng) were used as templates for real-time PCR using EXPRESS SYBR® GreenER™ qPCR supermix. qPCR was performed in the StepOnePlus real-time PCR system (Applied Biosystems).

Labeling, transplantation and drug treatment of PCa grafts in zebrafish

Wild type EKK, Casper and *AB zebrafish (*Danio rerio*) were maintained following an approved aquatic animal protocol. Adult fish were spawned and reared in conditioned water at 28.5°C on a 14-h-light 10-h-dark cycles. Embryos were staged as described (http://zfin.org). Quantum dots (QDs) labeled human PCa cells were tracked in embryos and juvenile Casper fish as described (6). Following initial imaging, transplanted embryos were maintained at 33°C for up to 12 days. Juvenile zebrafish at 6-8 weeks of age were immune-suppressed with 10μg/ml dexamethazone for 2 days as described (17). Xenografts were examined for QD fluorescence upon tumor formation and treatment, and equal numbers of QD positive cells from pooled primary grafts were used for injection into secondary recipients. Sections were examined for histological and IHC analyses and compared to primary tissues as described (6), and further details are provided in the Supplementary Methods.

Small molecular translation assay

Transcription and translation of BMI-1 *in vitro* was done utilizing the human BMI-1 cDNA. Briefly, the full length 3.2 Kb fragment of the human BMI-1 cDNA (containing 5‘UTR and 3‘UTR) was subcloned into the BamHI site of pSK+ downstream of the T7 promoter. The resulting pSK+-hBMI-1-cDNA vector was linearized with SacI, purified and utilized for TNT coupled transcription/translation systems (Promega) following the manufacturer's instructions. T7-mediated translation of mRNA (133 nM), after preincubation with or without 2μM C-209 for 60 min at 30°C was performed in cell-free reticulocytes lysates. Aliquots of the transcribed products were run on an agarose gel to confirm equal transcription. The newly synthesized proteins were analyzed on SDS-polyacrylamide gel electrophoresis and probed for BMI-1 expression using the rabbit monoclonal anti-BMI-1 (D20B7) antibody (Cell Signaling).

Treatment of mouse xenografts

Animal studies were performed according to Robert Wood Johnson Medical School IACUC protocol #I12-024-5. In order to differentiate tumor from contaminating non-tumor mouse cells, prior to mice injection, DU145 cells were infected with lentiviral vector encoding luciferase2/enhanced green fluorescent protein (Luc2/EGFP) that was generated as described (18). Luc2/EGFP cells were sorted (or enriched with the adherence assay) and CD49/CD29/CD44^{hi} cells were isolated, suspended in 100 μl mixed 1:1 with matrigel (BD Biosciences), and injected subcutaneously (SC) into the left flank of six week-old NOD SCID IL-2Rnull (NSG) mice. After tumor formation, mice were randomized and SC administered with docetaxel 6 mg/kg once per week for 2 weeks, or C-209 at a dose of 60 mg/kg daily for twelve days. Tumor growth was evaluated with an electronic caliper before

every administration, and measured every 3 days until day 30 and subsequently removed. Paraffin sections (5μm) of day 30 mouse xenografts were H&E stained and incubated with anti-Ki67 (Upstate-Millipore, Billerica, MA), -BMI-1 (Cell Signaling) and -CD44 (R&D Systems). To calculate retention of tumor-seeding capacity, tumor xenografts were dissociated following treatments, and recovered cells were sorted for EGFP. Equal numbers of EGFP positive cells were next re-injected into secondary recipients.

Statistical analysis

All statistical analyses were performed using GraphPad Prism 6 (GraphPad Software Inc). Data are presented as mean ± standard deviation (S.D.). Statistical significance was determined by student's t-test or ANOVA (one-way or two-way) with Bonferroni post-hoc test. Mann-Whitney U test was used to compare the differences in xenograft tumor volumes between two groups. A P value <0.05 is represented by a single asterisk, a P value <0.01 is represented by a double asterisk, three asterisks indicate P<0.001 while four asterisks indicate P<0.0001.

Results

BMI-1 is a potential target for human prostate TICs

BMI-1 is a key player in PCa initiation, recurrence and progression (11, 12). Accordingly, we found that BMI-1 is differentially expressed in PCa cell lines, but low in normal prostate epithelial cells (Supplementary Fig. S1*A*). To assess the functional role(s) of BMI-1 in PCa, we performed BMI-1 loss-of-function analyses in DU145 PCa cells (Supplementary Fig. S1*B*). Downregulation of BMI-1 was associated with decreased cell motility and clonogenic capability, as well as decreased cell survival, alone and when combined with chemotherapy (Supplementary Fig. S1*C*-*E*). Notably, resistance to drug-induced apoptosis, motility, invasiveness and clonogenicity have been traced to TICs (19).

We recently found that in PCa, clonogenic, migratory and *in vivo* tumorigenic potentials are enriched in the collagen-I rapidly adherent (5min) $CD49b^{hi}CD29^{hi}CD44^{hi}$ cell population (6), identified therefore as TICs. Thus, we utilized this functional adherence assay to analyze BMI-1 expression. Indeed, the rapidly adherent DU145 cells were enriched in the $CD49b^{hi}CD29^{hi}CD44^{hi}$ phenotype (Fig. 1*A* and *B*), and significantly overexpressed BMI-1, both at the RNA (Fig. 1*C*) and protein levels (Fig. 1*D* and *E* and Supplementary Fig. S2*A*). Furthermore, as expected, the rapidly adherent $CD49b^{hi}CD29^{hi}CD44^{hi}$ TICs were enriched for the other prostate TIC markers integrin-α6 (CD49f) and TROP; (4, 8) (Supplementary Fig. S2*B*), suggesting that BMI-1 is enhanced in the more tumorigenic cell compartment (6) of PCa. To confirm our results and model, we also assessed BMI1 expression upon sorting of the high and low CD49CD29CD44 cells and found the same outcomes (Supplementary Fig. S2*C*).

Thus, to study whether BMI-1 expression modulates the levels of TICs, we employed the collagen adherence assay after lentiviral-mediated knockdown. Loss of BMI-1 in sh-BMI-1 DU145 cells resulted in a significant (~40%) decrease in the numbers of rapidly adherent

CD49b^{hi}CD29^{hi}CD44^{hi} cells (Fig. 1*F*), suggesting an impact of BMI-1 on the TIC population.

Identification of pharmacological BMI-1 inhibitors

We previously demonstrated that BMI-1 expression is tightly controlled by post-transcriptional processes mapping to the 5'- and 3'-untranslated regions (UTRs) (14). In reporter cells containing the luciferase open reading frame flanked with the human BMI-1 5'- and 3'-UTRs, the BMI1 3′-UTR enhanced BMI-1 expression, while the internal ribosome entry site (IRES)-containing 5'-UTR impaired BMI-1 expression and controlled the effect of the 3'-UTR (14).

These observations allowed the construction of a platform to identify compounds impacting the regulatory mechanisms within the BMI-1 5'UTR and 3'UTR to modulate BMI-1 protein expression (14, 20).

A high-throughput screen against a library of >200,000 small molecules (PTC Therapeutics) identified seven compounds targeting the post-transcriptional control mechanisms described above (14, 20). To examine their antitumor activity, we determined their IC_{50} concentrations in DU145 cells (Supplementary Fig. S3*A*). Among them, three compounds: C-209, C-210 and C-211 significantly decreased the number of rapidly adherent and highly BMI-1 expressing CD49b^{hi}CD29^{hi}CD44^{hi} cells by an average of 30-50% (Fig. 2*A*). Accordingly, inhibition of proliferation was also observed following C-209 treatment in sorted CD49bCD29CD44 ^{hi} *vs* low cells (Supplementary Fig. S3*B*).

BMI-1 enables transcriptional repression of >1,600 target genes through the PRC1 complex (21), therefore, targeting BMI-1 would evoke complex cellular responses depending on the cell type and/or activated pathways. We evaluated BMI-1 protein inhibition by ELISA and Western blotting in comparison to EZH2; a closely related PRC2 protein with a similarly short half-life (22). Indeed, all three compounds reduced BMI-1 expression in a dose-dependent manner (Fig. 2*B* and Supplementary Fig. S3*C*), but had no effects on EZH2 levels (Supplementary Fig. S3*C*).

Furthermore, BMI-1 knockdown induces senescence (10). Treatment of mouse embryonic fibroblasts (MEFs), that are either Bmi-1$^{+/+}$ or Bmi-1$^{-/-}$, with C-209, C-210 and C-211 respectively, elicited a significant dose-dependent increase in senescence in Bmi-1$^{+/+}$ MEFs, and sh-BMI-1 DU145 cells, but not in the highly senescent Bmi-1$^{-/-}$ MEFs (Supplementary Fig. S3*D* and *E*). Accordingly, when we assessed β-Gal staining in CD49b^{hi}CD29^{hi}CD44^{hi} in comparison to CD49b^{low}CD29^{low}CD44^{low} cells, we observed in TICs a greater senescence following C-209 treatment, as expected in regard to a much higher BMI-1 expression in CD49b^{hi}CD29^{hi}CD44^{hi} cells (Supplementary Fig. 3*F* and *G*), thus suggesting a potential functional specificity of the selected inhibitors in targeting BMI-1's effects on cellular senescence.

Pharmacological targeting of BMI-1 in human prostate TICs

To establish that BMI-1 inhibitors have activity against the putative TICs in PCa, we treated different PCa cells with C-209. This treatment significantly impaired the percentage of

rapidly adherent CD49b^{hi}CD29^{hi}CD44^{hi} (TICs) (Supplementary Fig. S4*A* and *B*), induced a cell cycle accumulation (Supplementary Fig. S4*C*), which was anticipated from loss of BMI-1's cell cycle regulatory function(s) (23), reduced the number of cells in S phase (Supplementary Fig. S4*C*) and critically, evoked a dose-dependent reduction in both BMI-1 and C-terminal lysine-119 mono-ubiquitinated form of γ-H2A, a specific product of the BMI-1 PRC1 complex activity (23) (Supplementary Fig. S4*D* and *E*).

Self-renewal capacity is a distinguishing property of stem cells. Serial clonogenic spheroid assays estimate the frequency of TICs, especially after treatments (24). To evaluate the ability of these compounds to target serial clonogenic capacity, single cells collected from primary spheroids were plated in the presence of C-209, C-211 and two commonly used chemotherapies, methotrexate and doxorubicin. Unlike the initial slight inhibitory effects of methotrexate and doxorubicin, treatment with C-209 and C-211 considerably diminished the number of single cell-derived secondary, and more importantly tertiary spheroids (Fig. 2*C*). While methotrexate had no effect, the outcomes of C-209 and C-211 treatment were remarkable, as nearly a 10-fold reduction was observed (Fig. 2*C*). We therefore hypothesized that inhibiting BMI-1 might eliminate self-renewing, hence more tumorigenic cells, while chemotherapies only affect the proliferating transit-amplifying cells sparing the ones endowed with clonogenic capacities, and characterized by a lower proliferative kinetic. In line with this notion, serial spheroid formation in presence of the general protein biosynthesis inhibitor cycloheximide (CHX) (25), similar to chemotherapies, did not impact cells capable of self-renewal (Fig. 2*C*), thus strengthening our hypothesis.

Effects of BMI-1 inhibition on normal cells

When targeting TICs, an important concern is the effect on “normal” cell compartments. To assess the effect of BMI-1 inhibition on normal tissues, we initially used zebrafish embryos, valuable models for *in vivo* drug toxicity screening studies (26).

In toxicological assays, C-209, C210, and C-211 had no notable effects on zebrafish development at their respective IC_{50s} (Supplementary Fig. S5*A*). However, unlike C-209, higher doses of C-210 and C-211 impeded embryo hatching and caused embryo curling, thus suggesting narrow safety margins (Supplementary Fig. S5*A* and *B*). These data prompted us to dismiss C-210 and 211 inhibitors and focus on establishing the safety profile of C-209. To provide evidence that the effects of C-209 were not related to a general disruption of mRNA translation, zebrafish embryos were exposed in parallel to the universal protein inhibitor CHX (Supplementary Fig. S6*A*). CHX treatment resulted in developmental arrest and profound embryonic toxicity at low concentrations, while embryos treated with C-209 at 3μM survived and progressed normally throughout development (Supplementary Fig. S6*A*). Likewise, treatment of adult zebrafish with C-209, but not CHX, yielded no apparent impact on survival (Supplementary Fig. S6*B*).

To further assess C-209 adverse effects on normal mammalian tissues, BMI-1 inhibition was also tested on normal prostate epithelial RWPE1 cells by examining clonogenic potential pre- and post-C-209 treatment. While C-209 drastically reduced DU145 PCa colony formation, RWPE1 cells, showing an expected lower clonogenic proclivity than DU145 cancer cells, BMI-1 inhibition was mostly ineffective (Supplementary Fig. S7*A*).

Furthermore, because self-renewal of hematopoietic stem and progenitor cells (HSPCs) is vital for the sustained production of blood cells (10), we evaluated the clonogenic capacity of primary human $CD34^+$ HSPCs upon treatment with C-209 and observed no significant effect (Supplementary Fig. S7*B*). Additionally, treatment of mice with C-209 did not induce any anemia and/or thrombocytopenia, nor were histological changes observed in the bone marrow of treated *vs.* untreated mice (Supplementary Fig. S7*C*), suggesting that dosage limited targeting of BMI-1 would be selective in inhibiting the clonogenic potential of tumor *vs* normal stem cells.

C-209 could target post-transcriptional regulation of BMI-1

To gain insight into the mechanism of action of C-209 (Fig. 3*A*) against PCa, We assessed the electrostatic potential of C-209 (Fig. 3*B*), and then used the UCSF DOCK program to model the docking of C-209 to the human BMI 5′UTR RNA. The docking model suggests that C-209 could bind to pockets formed in the BMI-1 RNA fold structures (Fig. 3*C*). We next utilized the BMI-1 UTR luciferase reporter constructs previously used to demonstrate the regulatory roles of BMI-1 UTRs (14), to examine the effects of C-209 on cells harboring these BMI-1 UTR regulatory reporters. Indeed, C-209 treatment significantly reduced normalized luciferase expression in cells harboring the BMI-1 3‘UTR and reversed the BMI-1 expression inducing effects of the BMI-1 3‘UTR (14) in cells harboring both the BMI-1 5‘ and 3‘UTR (Fig. 3*D*). Thus, in PCa cells, C-209 engages the BMI-1 regulatory mechanisms embedded within the UTRs.

To examine if C-209 is selective for BMI-1 post-transcriptional inhibition, we utilized control and BMI-1 UTRs reporter cells and found that C-209 preferentially inhibit expression of a reporter, the translation of which is under the BMI-1 5‘- and 3‘UTR control, rather than alternate control UTRs (Fig. 3*E*). We also treated DU145 cells concomitantly with C-209 2μM and CHX, a general translational inhibitor, and analyzed mRNA expression of BMI-1 and the CHX target epithelial sodium channel (αENaC) (27). While treatment with CHX mutually lowered mRNA levels of both BMI-1 and αENaC, C-209 exposure did not exert a lowering effect on the levels of transcribed BMI-1 mRNA, explained by a reported cancer cellular addiction to BMI-1 (11, 12, 28). Thus, C-209 reduces the production of BMI-1 protein likely by modulating its post-transcriptional regulation.

Nonetheless, to specifically link C-209 effects to targeting post-transcriptional regulation of BMI-1 transcripts, we analyzed BMI-1 translation directed by full-length (UTR-containing) human BMI-1 cDNA (29) in eukaryotic cell-free expression system. Incubation of the BMI-1 cDNA with C-209 for just one hour before translation decreased BMI-1 protein synthesis by 27% (Fig. 3*F*).

Moreover, we performed a dose-response cell viability assay in BMI-1-deficient (sh-BMI-1) and BMI-1-overexpressing (EGFP BMI-1) DU145 cells, and compared the results to control transduced DU145 Sh-Scr cells expressing endogenous level of the protein (Fig. 3*G*). Unlike DU145 Sh-Scr cells, whose survival was impaired even at low C-209 doses (IC_{50} 1.25-2.5 μM), both DU145 BMI-1-deficient (lacking the target) and -overexpressing (with excess target) cells showed a lower sensitivity, being affected only at very high concentrations of C-209 (DU145 EGFP-BMI-1 IC_{50} ~10μM and DU145 sh-BMI-1 IC_{50} ~15μM). Survival

analyses comparison between DU145 Sh-Scr and DU145 sh-BMI-1 cells revealed a highly significant response of DU145 Sh-Scr cells to C-209 even starting at 0.3125 μM (Fig. 3*H*). Accordingly, in order to experience the growth-inhibitory effect of C-209, BMI-1-overexpressing cells required a higher dose than DU145 Sh-Scr (Fig. 3*H*), therefore providing additional evidence that C-209 effects could be selective towards BMI-1 targeting.

Also, to examine other potential mechanisms of action, C-209 inhibitory activity was examined against a panel of 245 kinases and 21 phosphatases. These assays elucidated a lack of significant inhibition (<10%) (data not shown).

BMI-1 inhibition in patient-derived TICs

To assess the value of a new treatment, primary patient-derived cells represent a much more relevant model compared to cell lines. Despite the known difficulties in culturing primary PCa cells *in vitro*, even if for brief periods, we have recently successfully maintained primary PCa cells endowed with self-renewal and *in vivo* tumorigenic potential in short-term culture (6). Therefore, we examined C-209 treatment in a panel of short-term cultures from primary PCa cells differentially expressing BMI-1 (Table 1 and Supplementary Fig. S8). Exposure of patient-derived PCa cells to C-209 resulted in significant BMI-1 downregulation (Fig. 4*A*) followed by antitumor activity at an IC_{50} similar to that found in androgen-responsive LNCaP cells and lower, but not significantly different, from the IC_{50} found in the androgen-insensitive DU145 cells (Fig. 4*B*). Notably, only a slight non-significant downregulation of BMI-1 was observed in patient-derived normal counterparts treated with C-209 (Fig. 4*A*). Remarkably, as observed with tumor cell lines, treatment with C-209 caused a critical reduction in the rapidly adherent $CD49b^{hi}CD29^{hi}CD44^{hi}$ (TIC) population in primary PCa cultures (Fig. 4*C*, left and right panels). In contrast, treatment with docetaxel, a treatment for advanced PCa (2), resulted in enrichment of the highly aggressive $CD49b^{hi}CD29^{hi}CD44^{hi}$ TICs.

The effectiveness of any targeted therapy is based on the absence of relapse and/or secondary clonal lesions (30). Since TICs account for tumor progression by the virtue of their treatment-resistance, self-renewal and tumor-seeding capacity (19), it is reasonable to deduce that the efficacy of a TIC-tailored strategy relies on a diminished clonogenic and tumorigenic capacity.

In order to evaluate C-209 efficiency in targeting patient-derived TICs, we pre-treated distinct unselected primary PCa cells for several days with either C-209 or docetaxel. Subsequently, to investigate the long-term impact of treatments, particularly in a post therapy discontinuation setting, cells were washed and replated. Cell rescue and soft agar assays were assessed to evaluate differences in cell survival and colony-forming repopulation abilities. Interestingly, both docetaxel and C-209 treatments impaired short-term survival of primary PCa, although C-209 to a more significant extent (Fig. 4*D*). Critically, patient-derived PCa cells maintained the ability to form colonies after single treatments with docetaxel but significantly less with C-209 (Fig. 4*E*), indicating that BMI-1 inhibition impairs survival and clonogenic activity of primary PCa TICs.

BMI-1 has been implicated in contributing to PCa metastasis (31). Since loss of function of BMI-1 impaired PCa cell migration (Supplementary Fig. S1*C*), we assessed the post-treatment propensity of patient-derived PCa cells to migrate in modified Boyden chambers. We found that, while docetaxel–treated cell migratory potential was almost unchanged, C-209-exposure significantly diminished their motility (Fig. 4*F*), thus suggesting a notable role for BMI-1 in cancer dissemination.

Evaluation of C-209 in vivo

Successful murine xenografting of primary human PCa, in the absence of inducing murine urogenital mesenchyme (32), has rarely been achieved. We have shown that embryonic and juvenile zebrafish could be successfully used as PCa xenograft models (6). Here, we utilized these xenografts to identify small molecule inhibitors that functionally target BMI-1 and self-renewal activities (Fig. 5*A*). We isolated PCa cells from twenty-four patients undergoing surgical prostatectomy (Table 1), and examined their tumor initiation potential in zebrafish xenografts (Supplementary Fig. S9*A*). PCas were diagnosed based on histological examination (Supplementary Fig. S9*B-D*). The expression of the PCa-specific alpha-methylacyl coenzyme-A racemase (AMACR) when combined with overexpression of Erg (33), provide excellent dual PCa-specific biomarkers (6) (Supplementary Fig. S9*E-G* and S10*A-B*). We detected Erg overexpression associated with AMACR in the mirror sections of sampled PCa tissue (Supplementary Fig. S10*E-G*), and within zebrafish xenografts (Supplementary Fig. S10*C-E*), in cells that expressed the human isoform of CD44 and BMI-1 (Supplementary Fig. S10*F-H*). TICs isolated from primary PCa engrafted robustly in the pre-immune zebrafish embryos (Supplementary Fig. S10*H*), forming xenografts (Supplementary Fig. S9*H-K*) with cells morphologically similar to the patient's biopsy cells (compare cells in Fig. S9*D* to those in Fig. S9*K*) and were positive for Prostatic Specific Antigen (PSA) staining (Supplementary Fig. S9*L-O*).

Again, we employed the zebrafish toxicity assay to demonstrate that the compounds under investigation have no notable toxicities when used at their corresponding IC_{50s} (Supplementary Fig. S11*A* and *B*). We next treated zebrafish embryos that were engrafted with quantum dot (QD)-labeled TIC-derived PCa (Fig. 5*A* and Supplementary Fig. S12*A*). Treatment of PCa xenografts from multiple patient samples (Fig. 5*B* and *C*) with C-209 at 2μM led to tumor shrinkage (Fig. 5*B* and *D* and Supplementary Fig. S12*B*, left and right panels). Likewise, treatment of juvenile xenograft fish with C-209 led to tumor reduction (Supplementary Fig. S12*C*, left and right panels), suggesting that although governing the cell fate of TICs, BMI-1 likely regulates the viability of PCa cells in general.

To determine C-209 efficacy in targeting TICs, hence tumor reinitiation, primary PCa were treated with either docetaxel or C-209 for three days before being washed and injected into zebrafish embryos. After 10 days, C-209-treated cells gave rise to significantly less tumors than control- or docetaxel-treated cells (Fig. 5*E*). Notably, these effects were associated with a significant reduction in Ki67 staining (Fig. 5*F*).

Xenotransplantation, followed by serial repopulation, is considered an essential criterion to assess serial maintenance of stemness in defining TICs. Thus, we sorted labeled pooled primary tumor cells from primary zebrafish xenografts treated either with DMSO or C-209,

and used them for secondary xenografts (Fig. 5*G*). TICs from DMSO-treated embryos were able to initiate secondary grafts in 81.8% of cases (n=54/66 secondary xenograft embryos from three patient samples), while C-209-treated cells had significantly less tumor initiation potential in only 29.3% of cases (n=22/75 from three patient samples) ($p<0.001$) (Fig. 5*G*), suggesting that C-209 treatment is effectively impairing the frequency of TICs in zebrafish xenografts.

Zebrafish provide a powerful organism to study the cancer self-renewal population (34). To examine whether C-209 treatment affects tumor response and TIC survival in a murine model, we employed a strategy aimed at unraveling the targeting of self-renewing TICs (Fig. 6*A*). We injected rapidly adherent $CD49b^{hi}CD29^{hi}CD44^{hi}$ DU145 TICs (6), that were previously infected with a lentiviral vector encoding luciferase2/enhanced green fluorescent protein (Luc2/EGFP), into NOD-SCID-IL-2R null (NSG) mice. Tumors, allowed to grow until the size of ~100 mm^3, were treated with C-209 or the chemotherapeutic agent docetaxel for ~2 weeks (Fig. 6*B*). At the end of treatments, while vehicle-treated tumors grew exponentially and docetaxel exerted a minimal effect on xenografts growth, C-209-treated tumors were significantly inhibited (Fig. 6*B*). Additionally, since tumor relapse is frequently observed following treatment discontinuation, tumor volume was monitored with an electronic caliper for additional 15 days. Noticeably, at the end of this period, the results in Fig. 6*B*, while revealing a significant difference in tumor growth between docetaxel-treated and untreated mice, show an even higher disparity in C-209-treated xenografts. In line with this, Ki67+ cells in grafts with reduced nuclear BMI-1 and surface CD44 expression from C-209 treated mice were significantly lower when compared to controls (Fig. 6*C* and *D*). Also, severe tumor damage, indicated by large necrotic areas and scarce cellularity, was present two weeks after the last delivery of chemotherapy and BMI-1 inhibitors (Supplementary Fig. S13) thus, corroborating the efficiency of anti-BMI-1-based therapy. Furthermore, the same outcomes were observed when treatments were performed on unsorted androgen-independent DU145 cells or androgen-dependent 22rv1 cell xenografts (Supplementary Fig. S14). In both mouse xenografts, C-209 showed tumor growth inhibition and lastly regression; although sooner and to a higher extent in androgen-independent DU145 cell (with relatively higher BMI-1 expression) xenografts (Supplementary Fig. S14).

To investigate whether C-209 treatment was able to target TICs *in vivo,* clonogenic assays *ex vivo* and serial transplantations were assessed from treated and untreated xenografts (Fig. 6*A*). Interestingly, the clonogenic potential of cells derived from C-209-treated tumors was significantly reduced (Fig. 6*E*). To determine the frequency of cells having clonogenic, hence tumorigenic function, in the mixed tumor bulk population, we performed *ex vivo* a limiting dilution assay between C-209-treated and untreated xenograft-derived cells. While control-derived cells were highly clonogenic, C-209-treated xenograft-derived cells generated colonies at a lower frequency (Supplementary Fig. S15). Importantly, while both control- and docetaxel-xenograft derived cells could be serially transplanted in secondary recipients, the graft repopulation capacity of C-209-treated tumors was significantly reduced (Fig. 6*F*), hence demonstrating that BMI-1 targeting is effective against tumor-propagating cells.

Clinical management of advanced PCa remains a challenge. To gain insights into the clinical relevance of BMI-1 inhibition, we treated androgen-responsive LNCaP and 22rv1 cells (Fig. 6*G* and Supplementary Fig. S16) and androgen-insensitive DU145 cells with C-209 (Fig. 6*G*). We observed that, compared to current standard of care treatments (docetaxel, enzalutamide and abiraterone), C-209 was more significantly effective in inhibiting cell growth, in both androgen-dependent and -independent cells (Fig. 6*G* and Supplementary Fig. S16*A*, left panel). Furthermore, when cells resistant to these therapies were subsequently treated with C-209, not only cell survival was strongly impaired, but more importantly, clonogenic activity was completely abrogated (Fig. 6*H* and Supplementary Fig. S16*A*, right panel and S16*B*).

Collectively, our data demonstrate that C-209, a novel small molecule that targets post-transcriptional regulation of BMI-1, displays anti-TICs and antitumor activities in both zebrafish and mouse PCa xenografts.

Discussion

Mounting evidence support the notion that distinct tumor subpopulations termed cancer stem cells (CSCs) or TICs as responsible for tumor generation and treatment failure (35, 36). Accordingly, to achieve tumor eradication, new approaches capable of targeting the tumorigenic core of cancers are needed. TICs possess indefinite replicative ability due to an inherent or acquired self-renewal capacity. Consequently, targeting self-renewal potential of a given tumor may be the key towards developing more effective treatments.

Here, we initially demonstrated that knockdown of BMI1 impairs stem cell-like traits in PCa, likely by reducing TICs frequency. Next, through high-throughput followed by selective approaches, our group was first to identify small molecules that targets BMI-1 post-transcriptional regulation (37), and here, we investigated the ability of the prototype molecule C-209 to interfere with PCa cell survival and self-renewal, similar to the effects in colon cancer (38).

Human prostate spheroids have increased BMI-1 (39). Herein we showed that, in the 5min adherent $CD49b^{hi}CD29^{hi}CD44^{hi}$ tumorigenic stem-like cells, BMI-1, Integrin-α6 (CD49f) and TROP2 levels are higher than in the non-tumorigenic counterpart. Moreover, BMI-1 protein is highly enriched in these 5min adherent $CD49b^{hi}CD29^{hi}CD44^{hi}$ cells. Colony, serial spheroid formation and tumor xenograft studies showed that BMI-1 controls self-renewal, hence tumor-seeding capacity of prostate TICs. Importantly, the same outcomes were not observed with conventional chemotherapies or general translational inhibitor treatments. These data suggest that, unlike chemotherapies, which largely spare cells endowed with tumorigenic capacities (35), exposure to C-209 efficiently reduces the survival and clonogenic potential of TICs in PCa.

Multiple molecular pathways regulate the self-renewal potential of stem cells and are therefore potential targets in TICs (40). Among these, BMI-1, the key component of PRC1 transcriptional repressor complex that plays important roles in cell cycle regulation and cellular senescence, represents a critical target. BMI-1 is in fact also necessary for Hh- (41),

β-catenin- (42), and Akt-mediated self-renewal (28, 43), thus is a key stem cell self-renewal regulator (43). In PCa, BMI-1 activation occurs in primary tumors (31), transgenic mice (11, 28), in stem cells from metastatic PCa with poor prognosis (13), and is highly predictive of PSA recurrence (12).

A possible drawback for the development of agents targeting stem cell self-renewal may be the potential toxicity deriving from inhibition of normal differentiation, particularly in HSPCs (44). Importantly, C-209 had less of an effect on $CD34^+$ HSPCs. The *in vivo* administration of C-209 did not alter bone marrow integrity, nor did it induce anemia and/or thrombocytopenia in treated mice. Additionally, no notable toxicity was observed in zebrafish at the tumor IC_{50} employed. These findings suggest that it might be possible to target TICs overexpressing BMI-1 with potent targeted therapy, and without notable toxic effects on normal cells. Indeed, we have recently demonstrated that lower (more tolerated) doses of AKT-targeted therapy could target and radiosensitize glioblastoma TICs overexpressing BMI-1 (43).

C-209 was identified in a screen utilizing reporter cells that harbor BMI-1 5‘UTR and 3‘UTR (37). Treatments of tumor cells with C-209 reduced BMI-1 protein levels but not EZH2 nor a panel of 245 kinases and 21 phosphatases, increased cellular senescence, reduced the specific BMI-1 product of activity lysine-119 mono-ubiquitinated form of γ-H2A (23), induced a cell cycle accumulation, and impaired TICs by abolishing serial spheroid formation *in vitro* and graft repopulation potential *in vivo,* altogether are functional effects suggesting that C-209 may directly or indirectly target BMI-1 to evoke a complex cellular response.

Structure activity relationship in UTR reporters and modeling studies suggest that C-209 is relatively selective towards targeting the BMI-1 transcript, harboring the BMI-1 UTR regulatory elements. Thus, the anti-proliferative effects of C-209 could be due to direct modulation of BMI-1 post-transcriptional control mechanisms regulating BMI-1 translation and embedded within the UTRs, such as control of translation initiation either directly in a cap-independent fashion or possibly through riboswitches, which not only control gene expression through the 5‘UTR, but also control splicing in the 3‘UTR by coupling metabolite binding to mRNA processing, or indirectly by regulating mRNA stability (45). Few small molecules elicit their effects by modulating RNA function(s) outside of the bacterial ribosome. As the exact site(s) on the BMI-1 5‘UTR and/or 3‘UTR targeted by C-209 remains to be determined, detailed biophysical and RNA binding affinity studies are necessary to delineate the exact selectivity of C-209 towards BMI-1 RNA.

ChIP-Seq and global mapping revealed that BMI-1 transcriptionally represses ~1,600 targets through the PRC1 complex, with many targets involved in apoptotic and cell survival pathways, therefore driving the proliferation-promoting function of BMI-1 (46). We observed that C-209 treatment interruption led to a rapid tumor growth rebound. Notably, BMI-1 inhibition affected both androgen-dependent and -independent PCa cell proliferation and inhibited *in vivo* tumor growth.

ADT has been the standard care for patients with advanced PCa. Although ADT shows clear benefits for many patients, castration-resistant prostate cancer (CRPC) inevitably occurs. Moreover, despite the initial effectiveness of second-generation AR directed therapy with abiraterone and enzalutamide, resistance to these agents develops in patients with CRPC. ADT, abiraterone, and enzalutamide stimulate TIC expansion by multiple pathways that drive resistance to these therapies (2). Notably, BMI-1 targets are associated with lethal therapy-resistant PCa (13). We demonstrate that, following C-209 exposure, both cell survival and clonogenic capacities are strongly impaired in chemo- or AR directed therapy treated-PCa cells. These effects were observed regardless of their hormonal dependence. Although, and in line with correlation of BMI-1 overexpression with PCa progression (12), targeting BMI-1 with C-209 was more effective in hormone-independent cells. Notably the efficacy of BMI-1 inhibition in androgen-independent cells did not change with the presence of previous treatments. Accordingly, while targeting of TICs should complement the current androgen- and proliferation-based approaches, BMI-1 inhibition monotherapy could possibly be attempted as a therapeutic approach to target therapy resistant PCa in the clinic.

We found BMI-1 to be overexpressed in secondary tumor lesions, also BMI-1 inhibition was accompanied by reduced cell motility in PCa, therefore a link may exist between BMI-1-expressing self-renewing TICs and cancer dissemination in PCa. Genetic modulation of BMI-1 in PCa cell lines revealed a linear correlation between protein expression and the anti-proliferative as well as anti-TIC response to C-209. Instead, tumors from different patients exhibit variable responses, due to their extensive heterogeneity (47) that, unlike immortalized cell lines (48), are derived from distinct genetic alterations and cell proliferation kinetics. Mutations, such as those affecting AR signaling and PTEN/PI3K/AKT activation, could render PCa cells addicted to the activity of BMI-1 signaling (28). The defects in Bmi-1 null mice are caused by inappropriate Ink4a/Arf expression (11). The proteins $p16^{Ink4a}$ and $p19^{Arf}$, which induce cell-cycle arrest and apoptosis through activation of Rb and p53, respectively, are not expressed in normal tissue but induced upon oncogenic signaling (49). Addiction of PCa cells to BMI-1 likely activates cellular signals in tumor cells, which are absent in normal tissue, to elicit aberrant proliferative and anti-apoptotic effects. This could explain the distinct cellular responses to BMI-1 inactivation among normal and tumor cells. The robust expression of BMI-1 in most PCa samples analyzed, the extreme sensitivity of PCa cells to BMI-1 inactivation vs normal cells, upregulation of BMI-1 mRNA as an initial response to C-209 treatment, all suggest that PCa cells might have an oncogenic dependence over BMI-1 activity, possibly through increased transcriptional self-regulation, and similarly to the oncogenic addiction to Myc (50). This dependence distinguishes TICs from normal cells and can be viewed as a survival mechanism, to maintain cancer cell viability, which could be exploited for targeted therapy. Overall, our data suggest that PCa cells are more sensitive to BMI-1 inhibition, corroborating similar preferential sensitivity of PCa *vs* normal tissues to BET domain inhibitors (50). We conclude that the identification of molecules targeting BMI-1, a self-renewal target involved in oncogenic addiction, may open new avenues to directly target TICs for PCa treatment while preserving normal stem cell populations.

Supplementary Material

Refer to Web version on PubMed Central for supplementary material.

Acknowledgements

We thank Drs. Maarten van Lohuizen (The Netherlands Cancer Institute) for the Bmi-1 knockout mouse embryonic fibroblasts (MEFs), and Leonard Zon (Harvard) for the Casper zebrafish. We thank Dr. David Augeri and members of his laboratory at the Department of Chemistry at Rutgers University for the synthesis and purification of the small molecules utilized in this study. This project was supported by the Department of Defense Grants (W81XWH-12-1-0249 to H.S.), National Cancer Institute (P30 CA072720 to R.D.), Rutgers Cancer Institute of New Jersey (Pilot Grant to J.B. and H.S.), Wellcome Trust grant (SDDI award # 092687) to PTC and New Jersey Health Foundation award (Innovation grant to H.S.).

References

1. Siegel RL, Miller KD, Jemal A. Cancer statistics, 2015. CA Cancer J Clin. 2015; 65:5–29. [PubMed: 25559415]
2. Attard G, Parker C, Eeles RA, Schroder F, Tomlins SA, Tannock I, et al. Prostate cancer. Lancet. 2016; 387:70–82. [PubMed: 26074382]
3. Collins AT, Berry PA, Hyde C, Stower MJ, Maitland NJ. Prospective identification of tumorigenic prostate cancer stem cells. Cancer Res. 2005; 65:10946–51. [PubMed: 16322242]
4. Goldstein AS, Lawson DA, Cheng D, Sun W, Garraway IP, Witte ON. Trop2 identifies a subpopulation of murine and human prostate basal cells with stem cell characteristics. Proc Natl Acad Sci U S A. 2008; 105:20882–7. [PubMed: 19088204]
5. Toivanen R, Berman DM, Wang H, Pedersen J, Frydenberg M, Meeker AK, et al. Brief report: a bioassay to identify primary human prostate cancer repopulating cells. Stem Cells. 2011; 29:1310–4. [PubMed: 21674698]
6. Bansal N, Davis S, Tereshchenko I, Budak-Alpdogan T, Zhong H, Stein MN, et al. Enrichment of human prostate cancer cells with tumor initiating properties in mouse and zebrafish xenografts by differential adhesion. Prostate. 2014; 74:187–200. [PubMed: 24154958]
7. Qin J, Liu X, Laffin B, Chen X, Choy G, Jeter CR, et al. The PSA(−/lo) prostate cancer cell population harbors self-renewing long-term tumor-propagating cells that resist castration. Cell Stem Cell. 2012; 10:556–69. [PubMed: 22560078]
8. Hoogland AM, Verhoef EI, Roobol MJ, Schroder FH, Wildhagen MF, van der Kwast TH, et al. Validation of stem cell markers in clinical prostate cancer: alpha6-integrin is predictive for non-aggressive disease. Prostate. 2014; 74:488–96. [PubMed: 24375374]
9. Kreso A, Dick JE. Evolution of the cancer stem cell model. Cell Stem Cell. 2014; 14:275–91. [PubMed: 24607403]
10. Park IK, Qian D, Kiel M, Becker MW, Pihalja M, Weissman IL, et al. Bmi-1 is required for maintenance of adult self-renewing haematopoietic stem cells. Nature. 2003; 423:302–5. [PubMed: 12714971]
11. Lukacs RU, Memarzadeh S, Wu H, Witte ON. Bmi-1 is a crucial regulator of prostate stem cell self-renewal and malignant transformation. Cell Stem Cell. 2010; 7:682–93. [PubMed: 21112563]
12. van Leenders GJ, Dukers D, Hessels D, van den Kieboom SW, Hulsbergen CA, Witjes JA, et al. Polycomb-group oncogenes EZH2, BMI1, and RING1 are overexpressed in prostate cancer with adverse pathologic and clinical features. Eur Urol. 2007; 52:455–63. [PubMed: 17134822]
13. Glinsky GV. Death-from-cancer signatures and stem cell contribution to metastatic cancer. Cell Cycle. 2005; 4:1171–5. [PubMed: 16082216]
14. Cao L, Bombard J, Cintron K, Sheedy J, Weetall ML, Davis TW. BMI1 as a novel target for drug discovery in cancer. J Cell Biochem. 2011; 112:2729–41. [PubMed: 21678481]
15. Pettersen EF, Goddard TD, Huang CC, Couch GS, Greenblatt DM, Meng EC, et al. UCSF Chimera--a visualization system for exploratory research and analysis. J Comput Chem. 2004; 25:1605–12. [PubMed: 15264254]

16. Patrawala L, Calhoun T, Schneider-Broussard R, Zhou J, Claypool K, Tang DG. Side population is enriched in tumorigenic, stem-like cancer cells, whereas ABCG2+ and ABCG2- cancer cells are similarly tumorigenic. Cancer Res. 2005; 65:6207–19. [PubMed: 16024622]
17. Sabaawy HE, Azuma M, Embree LJ, Tsai HJ, Starost MF, Hickstein DD. TEL-AML1 transgenic zebrafish model of precursor B cell acute lymphoblastic leukemia. Proc Natl Acad Sci U S A. 2006; 103:15166–71. [PubMed: 17015828]
18. Kokorina NA, Granier CJ, Zakharkin SO, Davis S, Rabson AB, Sabaawy HE. PDCD2 knockdown inhibits erythroid but not megakaryocytic lineage differentiation of human hematopoietic stem/progenitor cells. Exp Hematol. 2012; 40:1028–42. e3. [PubMed: 22922207]
19. Visvader JE, Lindeman GJ. Cancer stem cells in solid tumours: accumulating evidence and unresolved questions. Nat Rev Cancer. 2008; 8:755–68. [PubMed: 18784658]
20. Peltz SW, Welch EM, Trotta CR, Davis T, Jacobson A. Targeting post-transcriptional control for drug discovery. RNA Biol. 2009; 6:329–34. [PubMed: 19574739]
21. Meng S, Luo M, Sun H, Yu X, Shen M, Zhang Q, et al. Identification and characterization of Bmi-1-responding element within the human p16 promoter. J Biol Chem. 285:33219–29.
22. Dimri M, Bommi PV, Sahasrabuddhe AA, Khandekar JD, Dimri GP. Dietary omega-3 polyunsaturated fatty acids suppress expression of EZH2 in breast cancer cells. Carcinogenesis. 2009; 31:489–95. [PubMed: 19969553]
23. Chagraoui J, Hebert J, Girard S, Sauvageau G. An anticlastogenic function for the Polycomb Group gene Bmi1. Proc Natl Acad Sci U S A. 2011; 108:5284–9. [PubMed: 21402923]
24. Franken NA, Rodermond HM, Stap J, Haveman J, van Bree C. Clonogenic assay of cells in vitro. Nat Protoc. 2006; 1:2315–9. [PubMed: 17406473]
25. Obrig TG, Culp WJ, McKeehan WL, Hardesty B. The mechanism by which cycloheximide and related glutarimide antibiotics inhibit peptide synthesis on reticulocyte ribosomes. J Biol Chem. 1971; 246:174–81. [PubMed: 5541758]
26. Sipes NS, Padilla S, Knudsen TB. Zebrafish: as an integrative model for twenty-first century toxicity testing. Birth Defects Res C Embryo Today. 2011; 93:256–67. [PubMed: 21932434]
27. Migneault F, Boncoeur E, Morneau F, Pascariu M, Dagenais A, Berthiaume Y. Cycloheximide and lipopolysaccharide downregulate alphaENaC mRNA via different mechanisms in alveolar epithelial cells. Am J Physiol Lung Cell Mol Physiol. 2013; 305:L747–55. [PubMed: 24039256]
28. Nacerddine K, Beaudry JB, Ginjala V, Westerman B, Mattiroli F, Song JY, et al. Akt-mediated phosphorylation of Bmi1 modulates its oncogenic potential, E3 ligase activity, and DNA damage repair activity in mouse prostate cancer. J Clin Invest. 2012; 122:1920–32. [PubMed: 22505453]
29. Alkema MJ, Bronk M, Verhoeven E, Otte A, van 't Veer LJ, Berns A, et al. Identification of Bmi1-interacting proteins as constituents of a multimeric mammalian polycomb complex. Genes Dev. 1997; 11:226–40. [PubMed: 9009205]
30. Sabaawy HE. Genetic Heterogeneity and Clonal Evolution of Tumor Cells and their Impact on Precision Cancer Medicine. J Leuk (Los Angel). 2014; 1:1000124.
31. Berezovska OP, Glinskii AB, Yang Z, Li XM, Hoffman RM, Glinsky GV. Essential role for activation of the Polycomb group (PcG) protein chromatin silencing pathway in metastatic prostate cancer. Cell Cycle. 2006; 5:1886–901. [PubMed: 16963837]
32. Risbridger GP, Taylor RA. Minireview: regulation of prostatic stem cells by stromal niche in health and disease. Endocrinology. 2008; 149:4303–6. [PubMed: 18535102]
33. Chaux A, Albadine R, Toubaji A, Hicks J, Meeker A, Platz EA, et al. Immunohistochemistry for ERG expression as a surrogate for TMPRSS2-ERG fusion detection in prostatic adenocarcinomas. Am J Surg Pathol. 2011; 35:1014–20. [PubMed: 21677539]
34. White R, Rose K, Zon L. Zebrafish cancer: the state of the art and the path forward. Nat Rev Cancer. 2013; 13:624–36. [PubMed: 23969693]
35. Chen J, Li Y, Yu TS, McKay RM, Burns DK, Kernie SG, et al. A restricted cell population propagates glioblastoma growth after chemotherapy. Nature. 2012; 488:522–6. [PubMed: 22854781]
36. Schepers AG, Snippert HJ, Stange DE, van den Born M, van Es JH, van de Wetering M, et al. Lineage tracing reveals Lgr5+ stem cell activity in mouse intestinal adenomas. Science. 2012; 337:730–5. [PubMed: 22855427]

37. Bansal, N.; Campbell, N.; Medina, D.; Dipaola, RS.; Bertino, JR.; Sabaawy, HE. Proceedings of the 101st Annual Meeting of the American Association for Cancer Research. AACR; Washington, DC: Philadelphia (PA): 2010. Targeting Bmi1 in human prostate tumor initiating cells.. Abstract nr 4279

38. Kreso A, van Galen P, Pedley NM, Lima-Fernandes E, Frelin C, Davis T, et al. Self-renewal as a therapeutic target in human colorectal cancer. Nat Med. 2014; 20:29–36. [PubMed: 24292392]

39. Guzman-Ramirez N, Voller M, Wetterwald A, Germann M, Cross NA, Rentsch CA, et al. In vitro propagation and characterization of neoplastic stem/progenitor-like cells from human prostate cancer tissue. Prostate. 2009; 69:1683–93. [PubMed: 19644960]

40. Reya T, Morrison SJ, Clarke MF, Weissman IL. Stem cells, cancer, and cancer stem cells. Nature. 2001; 414:105–11. [PubMed: 11689955]

41. Liu S, Dontu G, Mantle ID, Patel S, Ahn NS, Jackson KW, et al. Hedgehog signaling and Bmi-1 regulate self-renewal of normal and malignant human mammary stem cells. Cancer Res. 2006; 66:6063–71. [PubMed: 16778178]

42. Bisson I, Prowse DM. WNT signaling regulates self-renewal and differentiation of prostate cancer cells with stem cell characteristics. Cell Res. 2009; 19:683–97. [PubMed: 19365403]

43. Mehta M, Khan A, Danish S, Haffty BG, Sabaawy HE. Radiosensitization of Primary Human Glioblastoma Stem-like Cells with Low-Dose AKT Inhibition. Mol Cancer Ther. 2015; 14:1171–80. [PubMed: 25695954]

44. Rizo A, Dontje B, Vellenga E, de Haan G, Schuringa JJ. Long-term maintenance of human hematopoietic stem/progenitor cells by expression of BMI1. Blood. 2008; 111:2621–30. [PubMed: 18156489]

45. Wachter A, Tunc-Ozdemir M, Grove BC, Green PJ, Shintani DK, Breaker RR. Riboswitch control of gene expression in plants by splicing and alternative 3' end processing of mRNAs. Plant Cell. 2007; 19:3437–50. [PubMed: 17993623]

46. Meng S, Luo M, Sun H, Yu X, Shen M, Zhang Q, et al. Identification and characterization of Bmi-1-responding element within the human p16 promoter. J Biol Chem. 2010; 285:33219–29. [PubMed: 20551323]

47. Barbieri CE, Bangma CH, Bjartell A, Catto JW, Culig Z, Gronberg H, et al. The mutational landscape of prostate cancer. Eur Urol. 2013; 64:567–76. [PubMed: 23759327]

48. Magee JA, Piskounova E, Morrison SJ. Cancer stem cells: impact, heterogeneity, and uncertainty. Cancer Cell. 2012; 21:283–96. [PubMed: 22439924]

49. Serrano M, Lee H, Chin L, Cordon-Cardo C, Beach D, DePinho RA. Role of the INK4a locus in tumor suppression and cell mortality. Cell. 1996; 85:27–37. [PubMed: 8620534]

50. Asangani IA, Dommeti VL, Wang X, Malik R, Cieslik M, Yang R, et al. Therapeutic targeting of BET bromodomain proteins in castration-resistant prostate cancer. Nature. 2014; 510:278–82. [PubMed: 24759320]

Statement of translational relevance

BMI-1 is associated with tumor initiation, progression, and resistance to therapy. We identified a class of small-molecule post-transcriptional inhibitors of BMI-1. BMI-1 inhibitors that target self-renewal of tumor initiating cells may be developed to treat specific cancers.

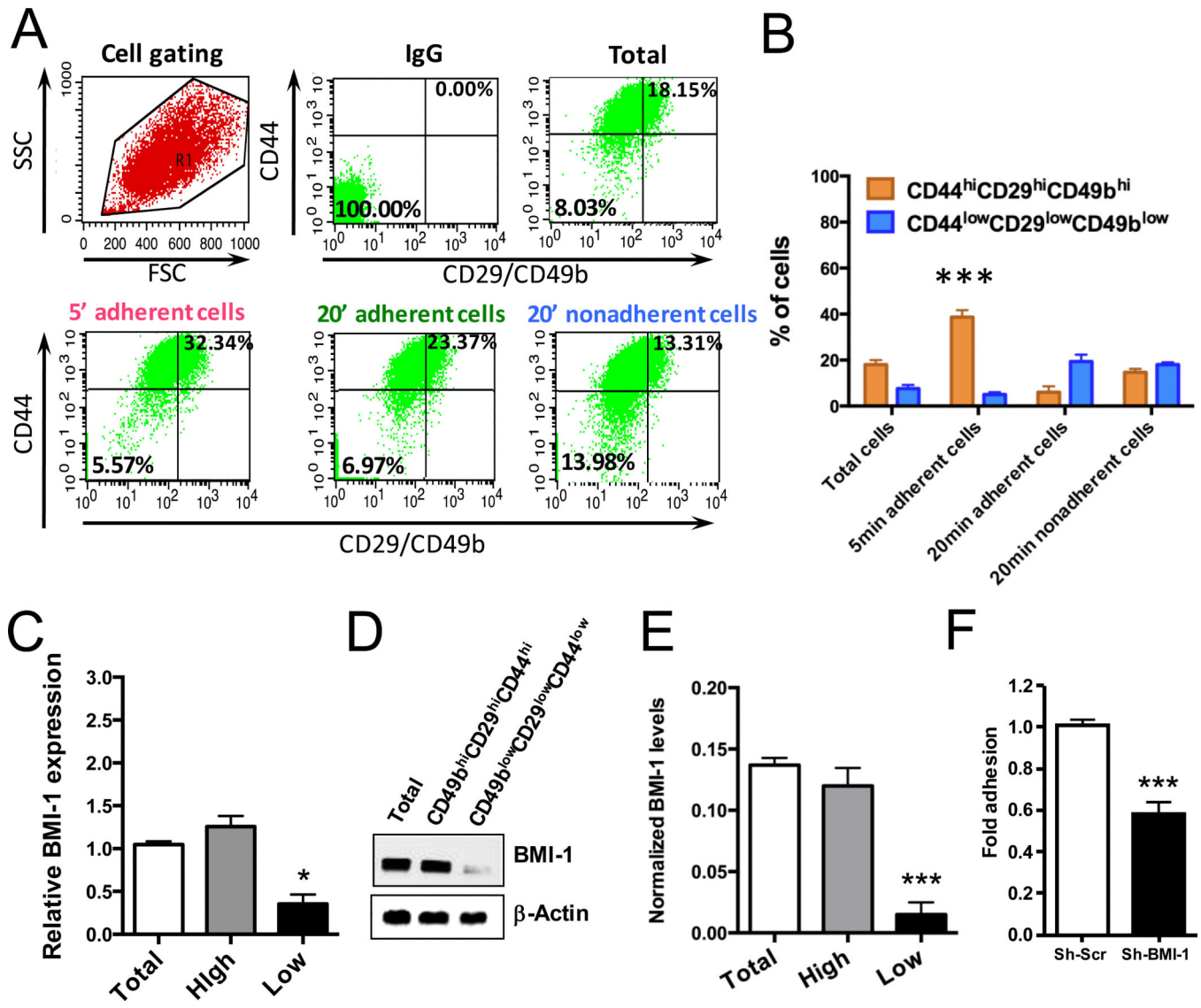

Figure 1.

Assessment of BMI-1 in PCa TICs isolated by combined adherence and phenotypic assays. *A,* Flow cytometric analyses. *B*, Percentage of cells identified by flow cytometry to express the TIC phenotype. *C*, Relative mRNA BMI-1 level in total, CD49b^{hi}CD29^{hi}CD44^{hi} (high) and CD49b^{low}CD29^{low}CD44^{low} (low) DU145 cells. *D*, Western blot analysis showing BMI-1 expression levels between total, CD49b^{hi}CD29^{hi}CD44^{hi} and CD49b^{low}CD29^{low}CD44^{low} DU145 cells. *E*, BMI-1 expression quantitation from 6 independent experiments. Anti-actin was used as a loading control. *F*, Fold adhesion of rapidly adherent CD49b^{hi}CD29^{hi}CD44^{hi} cells assessed over total DU145 control (Sh-Scr) and DU145 BMI-1-depleted (Sh-BMI-1) cells. Results are shown as mean ± S.D. of three independent experiments. **P-value <0.01, ***P-value <0.001.

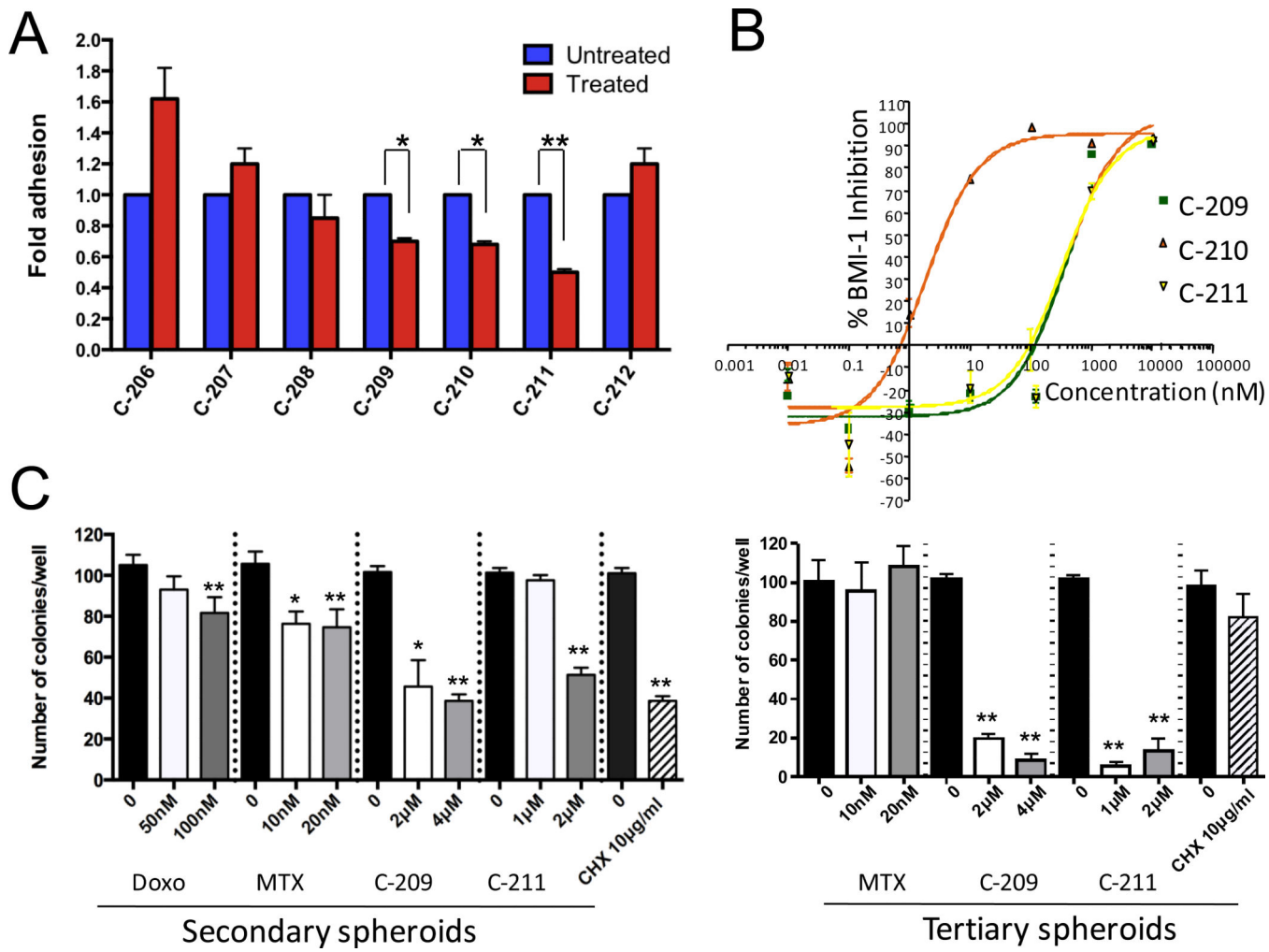

Figure 2.

BMI-1 inhibition reduces TIC number and interferes with self-renewal capacity *in vitro*. *A*, Fold adhesion of rapidly adherent CD49b^{hi}CD29^{hi}CD44^{hi} cells evaluated upon treatment of total DU145 with inhibitors targeting BMI-1 for 72hrs. *B*, IC_{50s} of compounds C-209-211 assessed in DU145 cells through an ELISA assay. *C*, Effects of BMI-1 post-transcriptional inhibitors vs. the non-specific protein translation inhibitor cycloheximide (CHX), or the chemotherapeutics methotrexate (MTX) and doxorubicin on secondary (left) and tertiary (right) prostate spheroids formation. Treatments that were statistically significant were indicated as *p <0.05 and **p<0.01, compared to untreated.

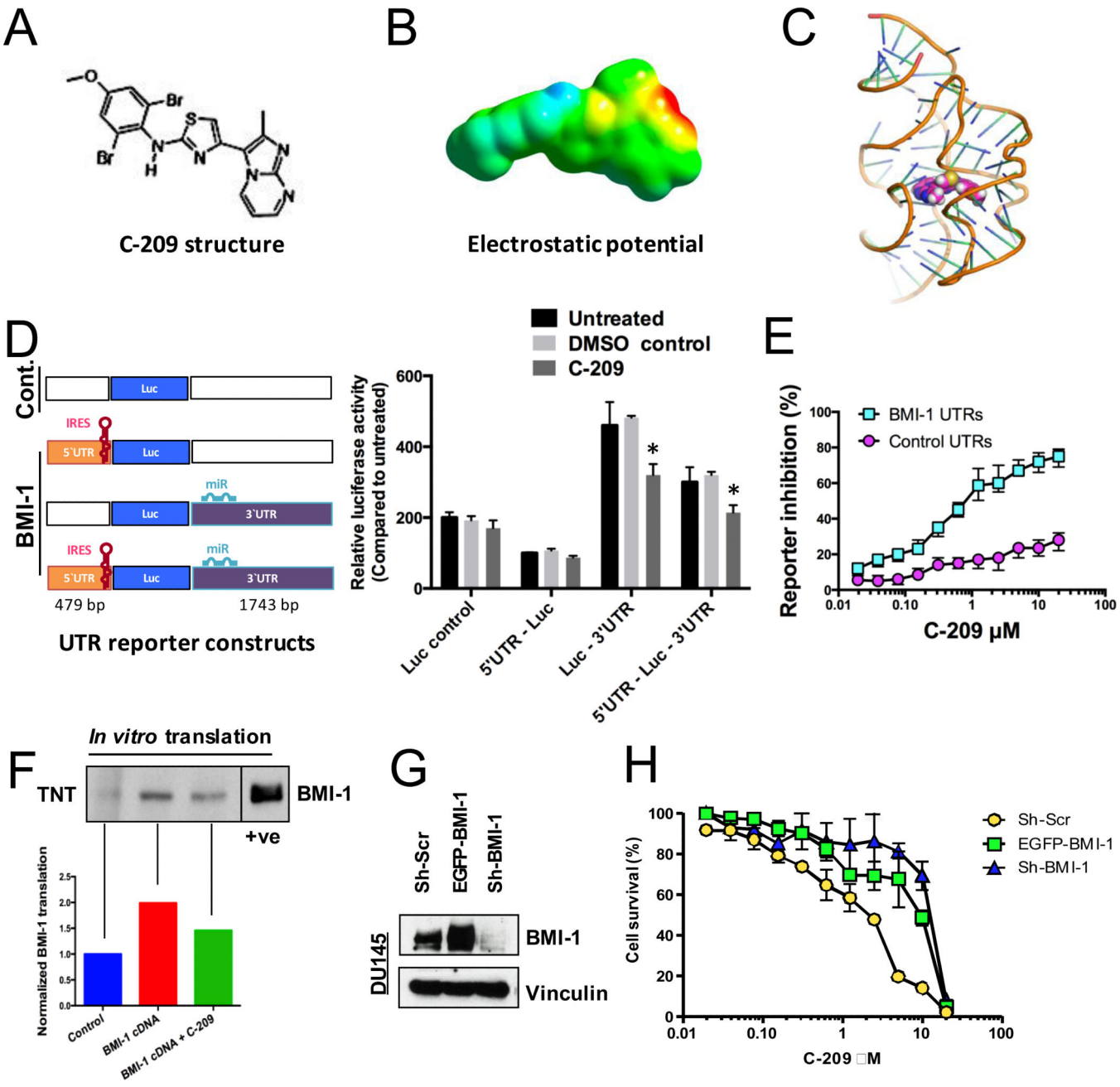

Figure 3.

Modulation of BMI-1 post-transcriptional regulation by C-209. *A*, Chemical structure of C-209. *B*, The electrostatic potential of C-209 mapped to electron density surface. At an IC_{50} of 2µM, the electrostatic potential E(RB3LYP) = −1423.42386733 au and dipole moment = 9.4906 Debye. *C*, Docking of C-209 to the human BMI-1 RNA. View of C-209 (space filling model colored magenta) within the binding pocket of the BMI-1 5‘UTR model (ribbon). Illustration was created using the Pymol software package. *D*, Left, Schematic diagram of the luciferase (Luc) constructs used. The diagrams display the IRES containing 5‘UTR and the micro-RNA (miR) binding sites within the 3‘UTR. The base pair (bp) length of the human BMI-1 5` and 3‘UTRs are displayed (from full length cDNA # L.13689.1).

Boxes and sites are drawn neither to scale nor to exact locations. Right, DU145 cells containing Luc flanked by control UTRs or BMI-1 5' or 3' UTR regions were treated for 24 hrs with 2μM C-209 and compared against untreated and DMSO controls. IRES-containing BMI-1 5'UTR and 3'UTR were shown to either inhibit or upregulate Luc expression, respectively (14). The 5'UTR reduced Luc expression, while when combined with the 3'UTR reversed the Luc expression enhancing effects of the 3'UTR. Treatment with 2μM C-209 resulted in reduced Luc expression opposing the effects of the 3'UTR. Data plotted represent six independent experiments. *E*, Percentage of inhibition of Luc reporter cells with either control (Cont.) vs. BMI-1 5' and 3'UTR cells following C-209 (0.0195-20μM) treatments for 72hrs. *F*, Selective effects of C-209 on BMI-1 mRNA translation in cell-free extracts. Top, WB analysis of translated full-length BMI-1 RNA (complete cDNA including BMI-1 5' and 3'UTRs) in *in vitro* transcription/translation (TNT) assays in eukaryotic cell-free rabbit reticulocytes. A cellular lysate in the left most lane was used as a positive control to determine the BMI-1 migrated band on the polyacrylamide gel at a position of ~37 KDa. Bottom, quantitation of normalized translated BMI-1 from BMI-1 cDNA pretreated or not with 2μM C-209 for one hour compared to control. *G*, BMI-1 expression in vector-transduced (Sh-Scr), BMI-1-overexpressing (EGFP-BMI-1) and BMI-1-depleted (shBMI-1) DU145 cells. *H*, Cell viability evaluated in vector-transduced (Sh-Scr), BMI-1-overexpressing (EGFP-BMI-1) and BMI-1-depleted (shBMI-1) DU145 cells following C-209 (0.0195-20μM) treatments for 72hrs.

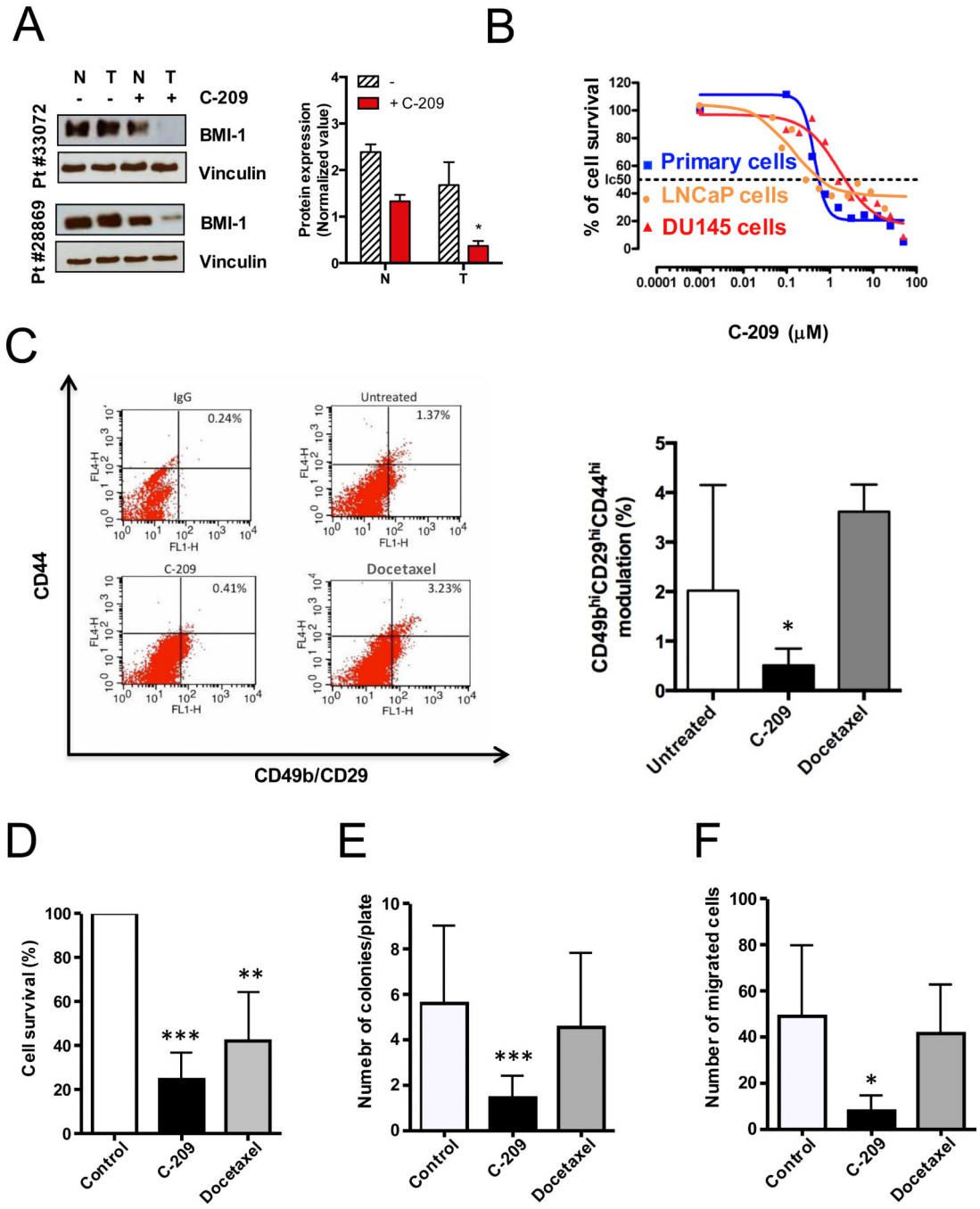

Figure 4.

Antitumor activities of C-209 against patient-derived TICs. *A*, BMI-1 expression levels assessed in normal (N) and tumoral (T) patient-derived samples before and after C-209 (2μM) treatment for 72hrs. Right panel. Quantitation of BMI-1 expression levels in normal (N) and tumoral (T) patient-derived cells after C-209 (2μM) treatment for 72hrs. *B*, Antitumor activity of C-209 in androgen-responsive LNCaP cells (orange), androgen-insensitive DU145 cells (red) and primary PCa cells (blue) (Patient#25854). Percentage of survival was evaluated by MTS assay. *C*, Representative cytofluorimetric analysis (left

panel) and graphical plotting (right panel) of TIC modulation in primary patient-derived cells untreated and treated with C-209 (2μM) and docetaxel (2.5nM) for 72h (Patient#28869, #33020, #33072, #33120, #33106).

D-F, Cell survival, clonogenicity and motility assessed on unselected primary PCa (#29084, #29092,#29110,#29663,#29834,#29990,#28869,#28864). Following treatments with DMSO, C-209 (2μM) or docetaxel (2.5nM) for 96hrs, cells were washed, counted and replated in fresh media to assess cell survival (assessed at 96h post cell wash), colony formation (assessed at 2-3 weeks post cell wash) and migration (24h post cell wash). Data are displayed as mean percentage ± S.D. Single independent experiments were performed with four to eight distinct patient-derived cells. *p <0.05, **p<0.01 and ***p<0.001.

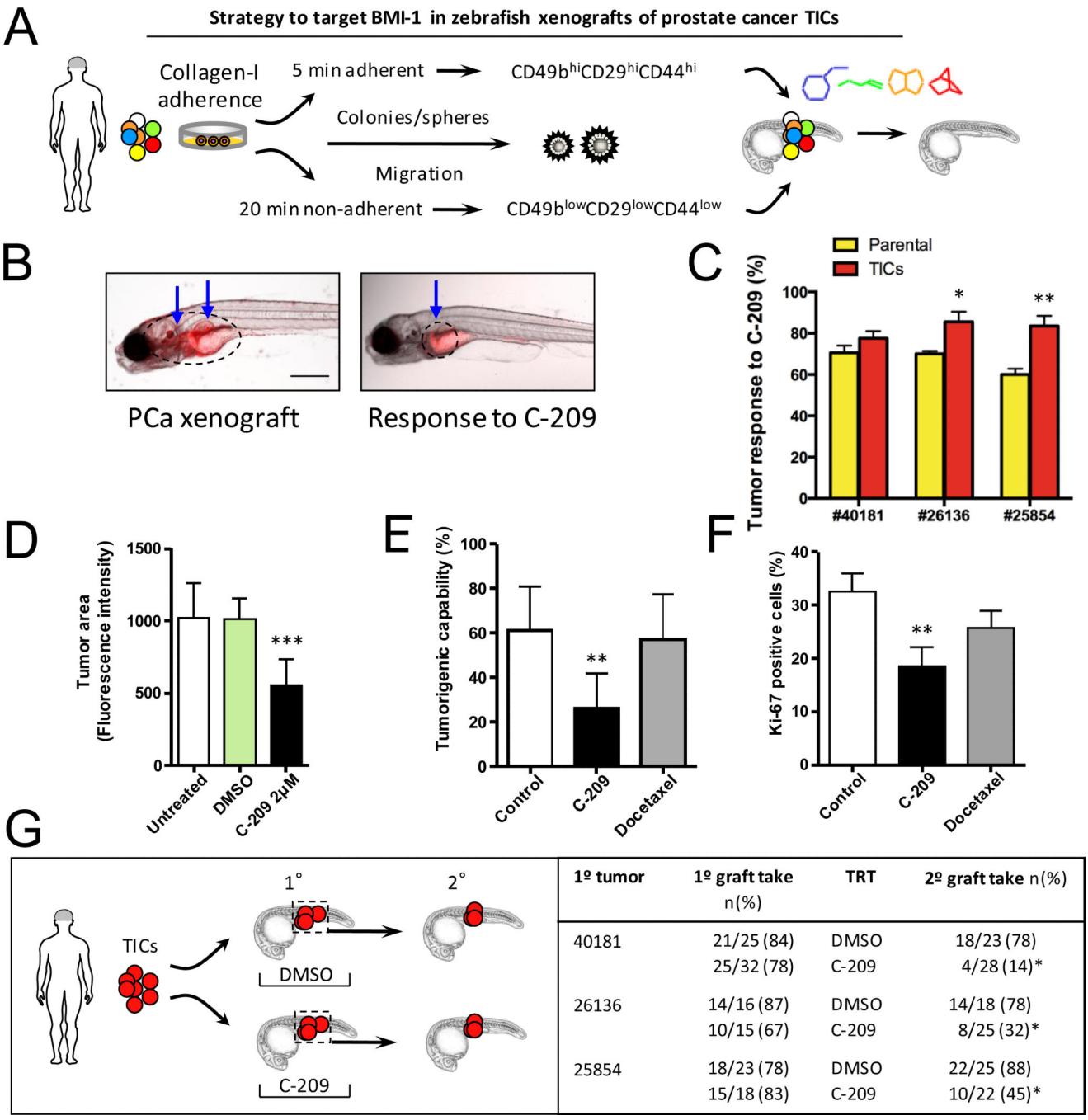

1º tumor	1º graft take n(%)	TRT	2º graft take n(%)
40181	21/25 (84)	DMSO	18/23 (78)
	25/32 (78)	C-209	4/28 (14)*
26136	14/16 (87)	DMSO	14/18 (78)
	10/15 (67)	C-209	8/25 (32)*
25854	18/23 (78)	DMSO	22/25 (88)
	15/18 (83)	C-209	10/22 (45)*

Figure 5.

Treatment effects of C-209 on zebrafish xenografts. *A*, Schematic illustration of the experimental procedure for the use of zebrafish PCa xenografts to identify small molecules targeting BMI-1 *in vivo*. *B*, Anti-tumor activity of C-209. Reduction in tumor size monitored with reduced QD fluorescence (blue arrows). *C*, Anti-tumor activity of C-209 (2μM) against xenografts derived from either parental cells (yellow) or the TIC fraction (orange) from three primary samples. The graph demonstrates responses to C-209 as a percentage of total treated xenografts (n=25 xenograft per cell fraction per patient). Zebrafish with established grafts

were sorted before treatment. *D*, Evaluation of tumor area variation calculated as fluorescence intensity of untreated and treated xenografts with C-209 (2μM). Data are presented as mean value ± S.D. *E*, Tumorigenic capacity of primary PCa TICs in zebrafish xenografts. Cells, pre-treated with C-209 (2μM) or docetaxel (2.5nM), were washed after 4 days, plated in fresh media for 3 days and subsequently injected in equal number into adult zebrafish. Data are displayed as mean percentage ± S.D. from four distinct patients (#29663, #29834, #29084 and #29990). *F*, The graph displays the percentage ± S.D. of Ki67 positive cells in DMSO (control), C-209 (2μM) or docetaxel (2.5nM) treated-cells. *G*, Strategy employed to determine inhibition of tumor initiation potential of remaining treated cells in secondary xenografts. TICs of patient samples #40181, #26136, and #25854 were transplanted to generate primary xenografts (1°). Diagram on the right demonstrates primary graft take rates. Xenografts were treated (TRT) with either DMSO or C-209 at 2μM for 72 hours, tumor areas were dissected, pooled, and TICs were sorted and injected into secondary recipients. Treatment with C-209 significantly reduced the rates of secondary xenografts (2°). Scale bars are 250 μm in *B* and 50 μm in *H*.

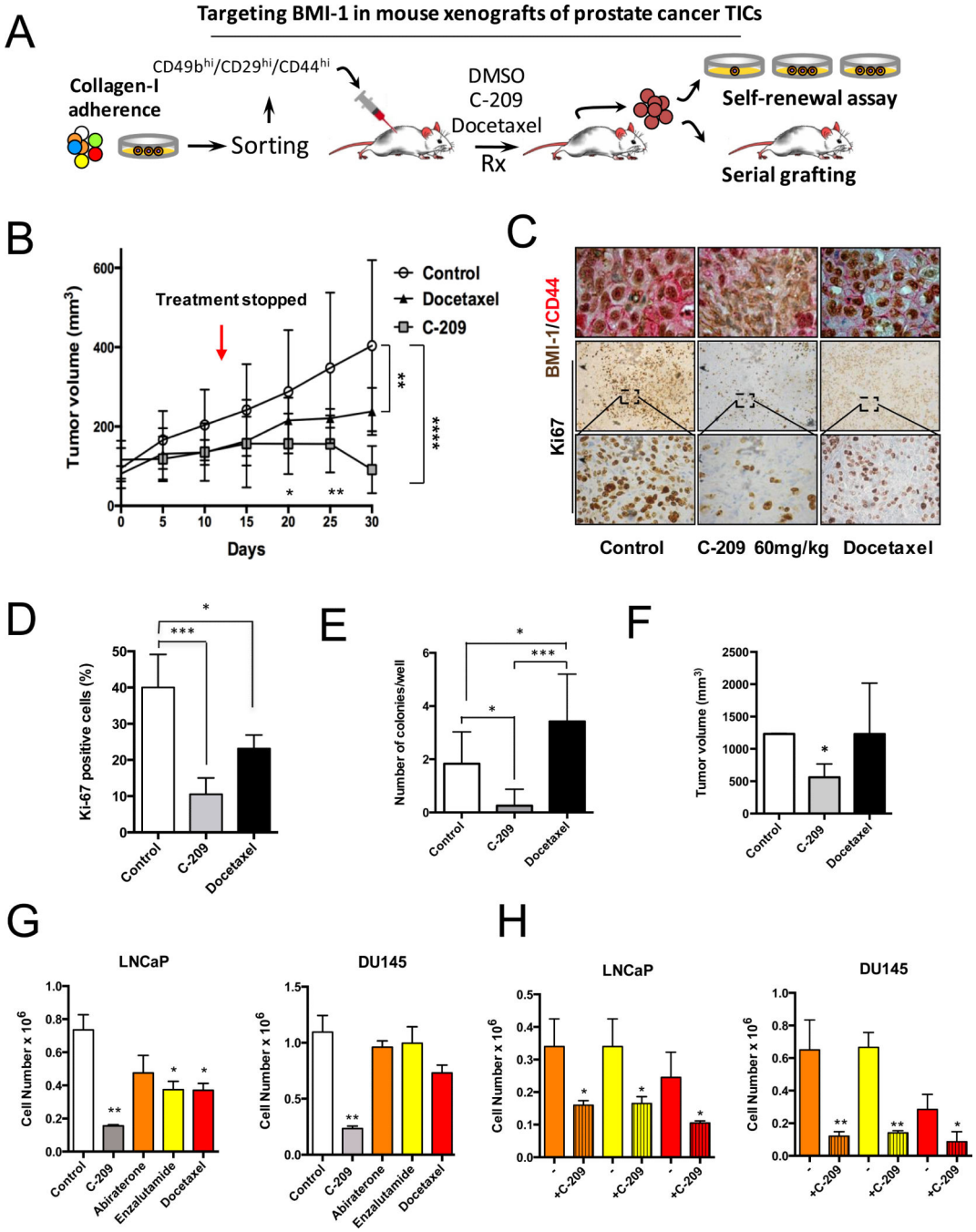

Figure 6.

In vivo pharmacological targeting of BMI-1 in mouse PCa xenografts. *A*, Strategy for examining the antitumor activity of C-209 in serial mouse xenografts and clonogenic repopulation assays of treated cells. *B*, Growth rate of mouse xenografts generated after subcutaneous (SC) injection of $CD49b^{hi}CD29^{hi}CD44^{hi}$ Luc2EGFP cells. Mice were randomized and administered daily with 60 mg/kg/day of C-209 for twelve days and docetaxel 6mg/kg once a week for two consecutive weeks. Results are mean ± S.D. of six independent experiments. Comparison of tumor volumes between the three groups was

determined by two-way ANOVA with Bonferroni post-hoc test. Graph indicates significance of Docetaxel *vs.* Control at day 30 (**p<0.01) and C-209 *vs.* Control at day 30 (****p<0.0001). There was a trend towards significance (p=0.08) when comparing tumor volumes in xenograft treated with C-209 *vs.* Docetaxel at day 30 using Mann-Whitney U test. At the earlier days 20 and 25, Docetaxel was not significantly different than Control, while C-209 was; C-209 *vs.* Control at day 20 (*p<0.05); C-209 *vs.* Control at day 25 (**p<0.01). Red arrow indicates treatment discontinuation. In each experiment, n=8/group. *C*, Intratumor IHC revealed reduced nuclear BMI-1 (brown) and surface CD44 (red) staining upon treatment with C-209. Staining was performed on tumor xenografts taken at Day 30. *D*, Quantitation of Ki67 positive cells in sections from treated xenografts. (***p<0.001, *p<0.01). *E*, Colony-forming ability assay performed on freshly dissociated and EGFP sorted xenograft-cells. Average number of colonies/plate for each treatment mean ± S.D. of two independent experiments with 12 wells/condition is reported. *p<0.05, ***p<0.001. *F*, Tumor initiation potential in serial grafting in secondary mouse xenografts of cells dissociated from treated primary mouse xenografts (n=8 mice /group, *p<0.01). *G*, Cell proliferation of LNCaP and DU145 cells treated with C-209 (2μM), abiraterone (5μM), enzalutamide (5μM) and docetaxel (2.5nM) for 72 hrs. *H*, Cell survival of therapy-resistant cells. LNCaP and DU145 cells pre-treated with abiraterone (5μM), enzalutamide (5μM) and docetaxel (2.5nM) for 72 hrs were washed and remaining cells that survived treatments (therapy resistant cells) were treated with C-209 (2μM) for another 3 days. Results are indicated as ± S.D. of two independent experiments with *p<0.05, **p<0.01.

Table 1

Primary prostate cancer patient characteristics.

Primary prostate cancer	Age	Type	Grade	pTNM	Gleason	BMI-1 expression by IHC
						H-score
15728	62	Adc	3	pT2c	3 + 3	120
17148	52	Adc	3	pT2c	3 + 3	150
17761	57	Adc	3	pT2c	3 + 3	ND
19803	55	Adc	3	pT2c	3 + 3	70
24126	53	Adc	4	pT3a	3 + 3	190
40181	60	Adc	4	pT3a	3 + 4	ND
25185	67	Adc	3	pT2c	3 + 3	200
25315	66	Adc	4	pT3a	3 + 4	150
26136	67	Adc	3	pT3b	4 + 5	220
25854	55	Adc	4	pT3b	4 + 5	190
28838	65	Adc	4	pT3b	4 + 4	160
28864	68	Adc	3	pT3b	3 + 4	210
28869	67	Adc	4	pT2c	4 + 4	200
29032	68	Adc	4	pT3b	4 + 5	210
29084	58	Adc	3	pT2c	3 + 3	ND
29092	71	Adc	4	pT3b	4 + 4	210
29110	69	Adc	4	pT3c	4 + 5	130
29663	50	mAdc	4	pT3b	4 + 5	250
29834	44	Adc	3	pT2c	3 + 4	160
29990	63	Adc	4	pT3a	4 + 3	200
33020	45	Adc	3	pT2c	3 + 4	165
33106	64	mAdc	5	pT3b	5 + 4	180
33072	48	Adc	4	pT3a	4 + 3	200
33120	47	Adc	3	pT2c	3 + 4	200

Table shows the de-identified number of each patient, age, prostate cancer type (Adc, adenocarcinoma, mAdc, metastatic adenocarcinoma), histological grade, pathological staging based on the pTNM classification, where pT2c indicates bilateral prostate disease, and total Gleason scores. BMI-1 expression is assessed as the extent of nuclear immunoreactivity by IHC and indicated as an H score. The H score is obtained using the following formula: H-Score = (% at 0) * 0 + (% at 1+) * 1 + (% at 2+) * 2 + (% at 3+) * 3. Scoring was determined as (3 X percentage of BMI-1 strongly staining nuclei + 2 X percentage of BMI-1 moderately staining nuclei + 1 X percentage of BMI-1 weakly staining nuclei), giving a range of 0 to 300. Weak cytoplasmic and/or stromal staining was seen in a few sections and was not considered in the score. BMI-1 staining in multiple sections from the same patient's tumor displayed marked heterogeneity. ND, not determined due to insufficient tissue material.